ACS OMEGA

Open Access

http://pubs.acs.org/journal/acsodf

Article

Highly Conductive Boron-Containing Electrolytes by Integrating Modeling and Experiments

Zuhair Hawsawi, Ahmed Alzharani, Duminda Samarakoon, Amal Abdulrahman, TaVeion Taylor, Md. Hanif Uddin, William Gladney, Xiao-Qian Wang,* and Ishrat Khan*

Cite This: *ACS Omega* 2025, 10, 127−133

Read Online

ACCESS | Metrics & More | Article Recommendations | Supporting Information

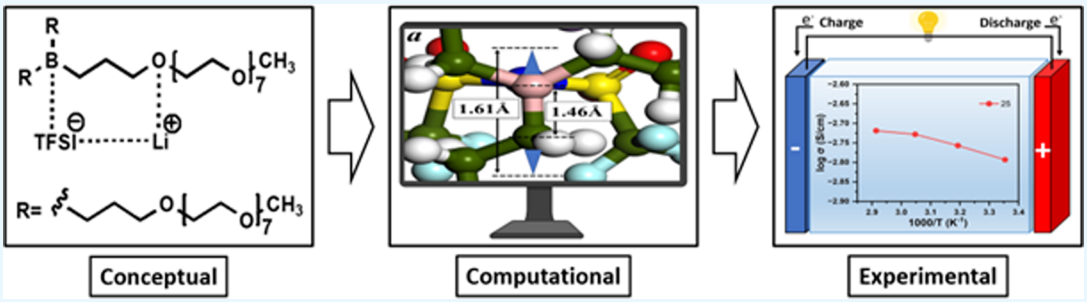

ABSTRACT: A highly conducting polymer electrolyte was developed, where the structure included molecular elements guided by computational modeling results. The electrolyte comprises acidic boron and basic oxygen atoms within the molecular structure. Because of the presence of the boron and oxygen atoms within the structure, it interacts with the anion and cation of the dissolved salt and functions as an ion separator by increasing the bond length between the anion and cation. Increasing the bond length weakens the electrostatic interaction between the anion and cation, resulting in a decreased level of aggregation within the electrolyte matrix and higher ionic conductance. The new electrolytes show ionic conductivity values of 10^{-3} S cm^{-1} at 25 °C, which are suitable for lithium-ion polymer batteries. The approach demonstrates the importance of integrating computational modeling with experimental studies to design and develop promising electrolytes for lithium-ion polymer batteries.

1. INTRODUCTION

Clean and renewable energy sources utilized at a higher level than currently used would minimize the adverse impact of using fossil fuels by reducing overall carbon emissions.[1−5] Consequently, the need to decrease dependence on fossil fuels and mitigate CO_2 emissions is of global interest and necessitates the development of effective and efficient high-energy-density power sources.[6−8] Promising energy storage devices are the lithium-ion battery (LIB) and the Li−air battery (LAB), which use lithium ions as the main component of their electrochemistry. Li batteries are rechargeable batteries commonly employed in portable electronic devices, electric vehicles, and aerospace applications.[5,6,9−13]

Polymer electrolytes used in lithium-ion batteries show low ionic conductivities for several reasons, including aggregation of the salts within the polymer matrix. In liquid and solid solutions of the electrolytes, the majority of the dissolved salts is present as dimers, tetramers, and higher aggregates. The aggregates are nonpolar compared with individually charged anions and cations and are in higher concentrations within the electrolyte matrix.[14,15] The formation of aggregates results in only a small fraction of the dissolved salts acting as mobile charge carriers. Furthermore, increasing the salt content increases the level of aggregation and does not necessarily contribute to additional charge carriers within the matrix. Within a polymeric electrolyte, there are multiple interactions, but to simplify the complex set of interactions, we may consider three interactions. The three interactions are the anion and cation interacting with the polymer backbone and the electrostatic interaction between the anion and the cation. Optimizing the three interactions may contribute to the design and development of new electrolytes with higher conductivity. Conceptually, controlling the interaction of the anion and cation with the polymer backbone may weaken the electrostatic interaction between the anion and the cation.

Most polymer electrolytes are based on poly(ethylene oxide)s, which can be explained based on the area's historical development. Interest in ion-conducting polymer electrolytes started in 1973 when Wright et al. demonstrated ion transport within poly(ethylene oxide)/alkali metal salt blends.[16,17]

Received: February 1, 2024
Revised: November 9, 2024
Accepted: November 15, 2024
Published: December 31, 2024

Scheme 1. Synthesis of Tripegylated Boron (TPB350) Structure

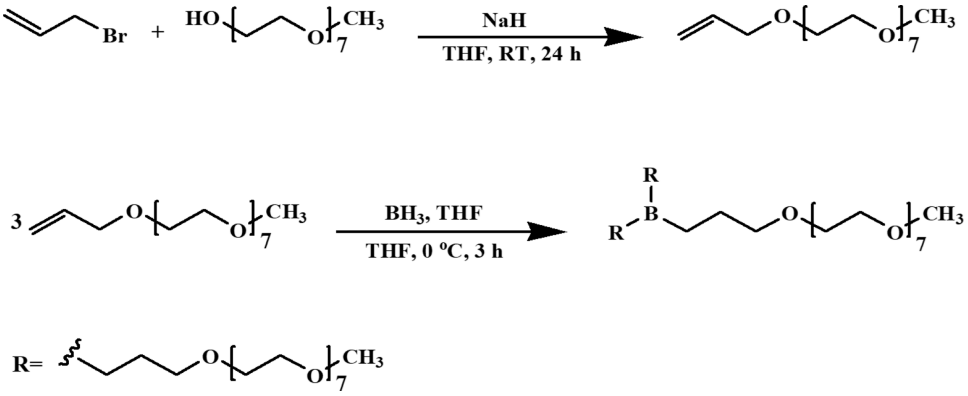

Wright's publications led to the design and development of many innovative, highly conductive electrolytes in the 1980s.[18−24] The reported electrolytes contained oxygen atoms interacting with the lithium cation and forming polymer salt complexes. It was determined in the 1980s that the segmental motion of the polymers facilitated ion transport within the electrolyte matrix. Thus, polymers with short oligooxyethylene side chains and low glass transition temperatures were synthesized. Two such polymers were the comb polymers of oligooxyethylene with polysiloxane and polyphosphazene backbones.[25,26] Modified versions of the siloxane polymers have since been reported.[23,27,28] One significant issue with these electrolytes was that the transference number of anions was high, and anion movement was the major contributor to the overall ionic conductivity value.[29,30] Therefore, to minimize anions' contribution to the observed ionic conductivity values, single-ion (cation) conducting polymers where the anion was covalently bonded to the polymer backbone have been reported.[31−33] Over the past four decades, numerous promising polymer electrolytes have been reported. Many of these electrolytes have excellent mechanical and conductive properties.[24]

As we develop newer electrolytes, perhaps we can prepare a structure that allows for controlling the interaction between the anion and the cation as well as the two interactions between the polymer backbone and the two ions. In ethylene oxide-based polymers, the oxygen atom coordinates with the lithium ion. In these polymers, because the anion is not coordinated with the polymer backbone, the anion becomes the dominant species, contributing to the overall ionic conductivity. Recent studies showed that cation diffusion could be increased by suppressing anion diffusion via Lewis acid sites.[34] The addition of different boron structures to electrolytes has been reported to anchor the anion and increase cation mobility.[35,36] An oligo(ethylene glycol) borate (OEGB) utilized as an anion-trapping material led to the dissociation of $LiClO_4$ by Lewis acid−Lewis base interaction between the boron atom of the OEGB and the ClO_4^- anion.[37]

In this report, we focus on three design requirements to develop a new electrolyte: (i) ion transport is a function of the segmental motion of the polymers, and thus, polymers with low glass transition temperatures are required; (ii) the polymer must have the ability to dissolve salts by acid−base interactions; (iii) the polymer contains both acids and basic sites.

2. EXPERIMENTAL SECTION

2.1. Materials. Supplies such as methoxypolyethylene glycol (MPEG, MW 350), THF, and allyl bromide were obtained from Sigma-Aldrich, purified, and dried before utilization. Sodium hydride (NaH) and anhydrous magnesium sulfate from Sigma-Aldrich were used as received, without additional purification. Borane tetrahydrofuran complex solution (1.0 M in THF) from Fisher Scientific was also used without further purification. Glassware was cleaned and dried in an oven before use.

2.2. Instrumentation. A Bruker 500 MHz nuclear magnetic resonance spectrometer (NMR) was employed for ^{1}H NMR analysis. Functional groups were identified by using a PerkinElmer L1600301 Spectrum Two FT-IR spectrometer. Thermal properties were examined by using a PerkinElmer differential scanning calorimeter (DSC 600) and a thermogravimetric analyzer (TGA 4000). Electrochemical properties were analyzed by using a 6430 SMU Keithley instrument.

2.3. Synthesis of Allyl-methoxy Polyethylene Glycol 350 (AMPEG). In a 250 mL three-neck round-bottom flask containing 100 mL of a dried THF solvent equipped with a magnetic stirrer, 10.9 g (0.03 mol) of MPEG 350 and 1.12 g (0.04 mol) of NaH were stirred under an inert atmosphere at 0−10 °C in an ice bath for 3 h. Then, 5.6 g (0.04 mol) of allyl bromide was added to the mixture, and the H_2 gas was evaluated. After that, the flask was capped with a rubber septum, and the reaction mixture was allowed to steer overnight at RT. Finally, the reaction mixture was filtered to remove the sodium bromide salt and the unreacted sodium hydride before removing the solvent using a rotary evaporator to yield 8.09 g (66%) of a slightly yellow oily liquid. The obtained product showed the following spectral results: FT-IR 1646 cm^{-1} (C═C), 3077 cm^{-1} (═C−H); ^{1}H NMR (500 MHz, $CDCl_3$) δ (ppm): 3.37 (3H, s, OCH_3), 3.50−3.81 (∼31H, m, OCH_2CH_2O), 4.01 (2H, d, ═$CHCH_2O$), 5.16 (1H, dd, and, H_{cis}C═$CHCH_2O$), 5.26 (1H, dd, H_{trans}C═$CHCH_2O$), 5.89 (1H, m, H_2C═$CHCH_2O$).

2.4. Synthesis of Tripegylated Boron (TPB). The reaction was carried out in a 100 mL three-neck round-bottom flask containing 25 mL of the THF solvent under inert conditions (Scheme 1). AMPEG (11.6 g, 0.03 mol) was added into the flask, and the mixture was flushed with N_2 gas for an hour. Then, 0.14 g (0.01 mol) of borane-tetrahydrofuran complex solution 1.0 M was added dropwise to the reaction mixture at 0 °C and allowed to stir overnight. After the reaction was stopped and the reaction mixture was filtered, the

https://doi.org/10.1021/acsomega.4c01051
ACS Omega 2025, 10, 127−133

solvent was removed by the rotary evaporator to yield 9 g (76%) of viscous oil. The product presented the following spectral results: FT-IR 1039 cm^{-1} (B−C); ^{1}H NMR (500 MHz, $CDCl_3$) δ (ppm): 1.35 (m, 2H, BCH_2C), 1.57 (m, 2H, $BCCH_2C$), 3.37 (s, 3H, OCH_3), 3.55 (m, 2H, $BCCCH_2O$), 3.60−3.78 (m, 32H, OCH_2CH_2O). ^{13}C NMR (125 MHz, $CDCl_3$) δ (ppm): 13.72, 18.79, 58.98, 67.92−70.49, 72.01.

2.5. Measurements. Ionic conductance was measured by the two-probe method[38] using a model 6430 SMU from Keithley with Remote PreAmp controlled by Lab Tracer software (Keithley Instruments, Inc.). A varying current was passed through the outer probes and induced a voltage in the internal voltage probes from −2.0 to +2.0 V. Resistance of the samples was determined using the two-probe method under nitrogen gas at 25, 40, 55, and 70 °C. The measurements were carried out during both the heating and cooling cycles. Each resistance measurement was repeated eight times. Conductivity measurements were carried out with the samples sandwiched between copper electrodes. Conductivity was calculated from the bulk resistance according to the following equation:

$$\sigma = (D/A) \times R$$

where σ is conductivity, D is the thickness of the sample, A is the section area of the sample, and R is bulk resistance.

3. RESULTS AND DISCUSSION

Instead of synthesizing various structures containing both acidic and basic sites, our approach started with computational methods so that we could narrow down possible structures to synthesize. Our study began with a first-principles analysis of boron centers' effects in polymer electrolytes using model molecules with three oligooxyethylene arms connected with a central boron or carbon atom (Figure 1). Energetic consequences of ion-pair dissociation and anion complexation at boron centers were calculated for LiTFSI. We calculated a 1:1 molecular ratio for the polymer and salt model complexes. The initial search for stable structures was done through force-field-based MD to obtain the optimum geometry and characterize the electronic interaction between PEO and LiTFSI. These energy minimizations were performed in vacuum. The resultant structures were further optimized through first-principles calculations. The binding energies were extracted from first-principles analyses.

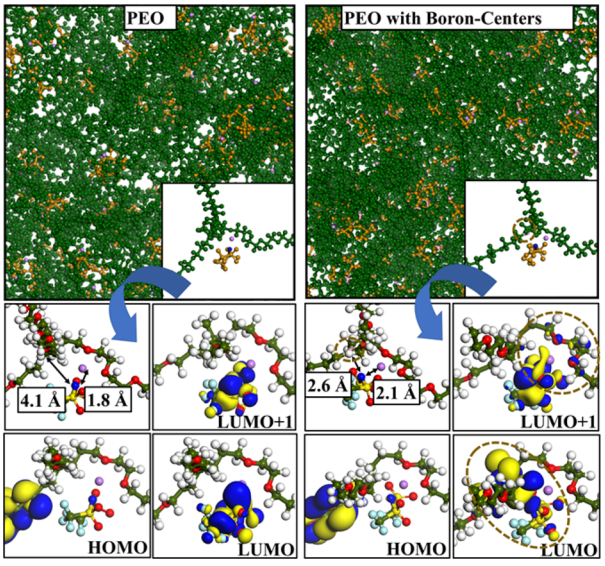

Figure 1. Depiction of the interactions in the polymer/LiTFSI electrolyte with (top right) and without (top left) a boron center. Insets show ion coordination without boron (bottom left panel) and with boron (bottom right panel). Elements are colored as follows: lithium (pink), fluorine (light blue), oxygen (red), carbon (green), and hydrogen (white). The polarized blue and yellow isosurface represents the calculated charge density at HOMO and LUMO levels (0.1 au).

After introducing boron centers, the calculation results reveal a reduction in binding energy between Li^+ and $TFSI^-$ (~29 kcal/mol per Li^+), i.e., the ionic bond strength between Li^+ and $TFSI^-$ decreased from 133 to 104 kcal/mol. As seen in Figure 1, the bond length between Li^+ and $TFSI^-$ increased from 1.8 to 2.1 Å after the addition of boron centers. Furthermore, the distance between the $TFSI^-$ and the polymer backbone decreased from 4.1 to 2.6 Å when the boron atom was part of the polymer structure. This suggests a strong interaction between the anion and the boron atom. In addition, the interaction between the nearest neighboring species of the nearest neighbor O and Li^+ increased. The distance between O and the Li^+ ions decreased from 2.5 to 1.9 Å after introducing boron centers. The increase in the bond length between the anion and cation and the decrease in the electrostatic interaction suggest that a structure containing both basic and acidic sites may function as an ion separator.

The charge density was calculated using first-principles density functional theory. As seen in Figure 1, the dashed brown circles in the LUMO and LUMO+1 highlight where the charge complexes are forming. The charge density distribution of LUMO+1 shows that a charged complex is formed between Li^+, $TFSI^-$, and the nearest neighbor oxygen in the polymer matrix after introducing a boron center. Thus, the charge density of the LUMO depicts the strengthening of interaction between the anion (TFSI) and the boron center. It is worth noting that the changes mentioned earlier in the charge density distribution are absent with the pure PEO polymer. Based on our modeling results, we synthesized the tripegylated boron structure shown in Scheme 1.

Allyl-methoxy polyethylene glycol 350 (abbreviated AMPEG 350) was synthesized using the reaction shown in Scheme 1. The characterization data for AMPEG are provided in the Supporting Information (Figures S1 and S2). The tripegylated boron, abbreviated as TPB350, synthesis was carried out by a dropwise addition of an excess amount of the boron/THF complex into a mixture of THF solution and allyl-methoxy polyethylene glycol 350 (AMPEG 350) at 0 °C. The reaction mixture was then stirred under N_2 gas at RT overnight. After that, the reaction mixture was filtered, and the THF solvent was removed by evaporating. These steps were repeated two more times to ensure that each of the B−H bonds of the BH_3 had reacted successfully with the alkene group of the AMPEG to form the TPB350, as shown in Scheme 1. One of the advantages of this reaction was that it could be carried out under mild conditions without any catalyst. Results of FT-IR spectroscopy of the obtained product show a band around 1045 cm^{-1}, corresponding to the stretching of the B−C bond (see Figure S3).

The ^{1}H NMR spectrum of the synthesized product displays peaks around 1.35 ppm, corresponding to ($B-CH_2$), and peaks around 1.57 ppm, related to ($BCC-H_2C$). The singlet peak at 3.37 ppm corresponds to the methyl group (CH_3-). The peaks around 3.55 ppm correspond to ($BCCCH_2O-$),

https://doi.org/10.1021/acsomega.4c01051
ACS Omega 2025, 10, 127−133

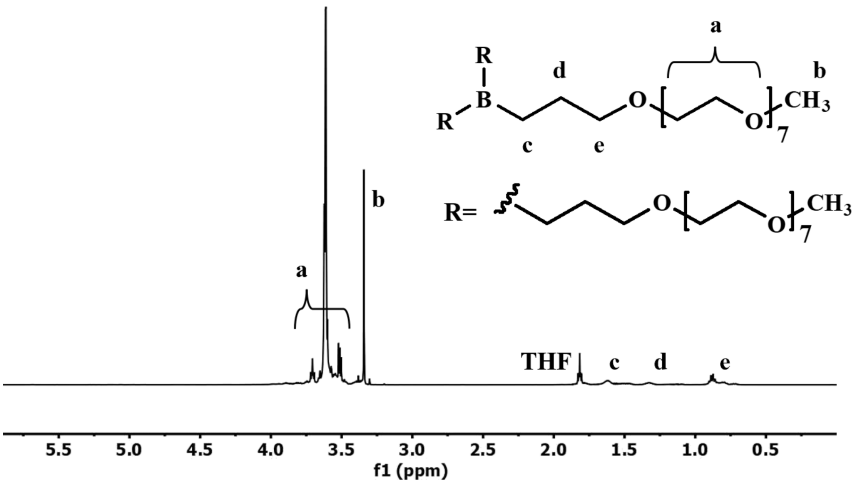

Figure 2. 500 MHz ^{1}H NMR spectrum of TPB350 in $CDCl_3$.

whereas those around 3.64 ppm correspond to ethylene oxide (CH_2CH_2O) repeating units, as shown in Figure 2.

The preparation of polymer electrolytes was conducted by mixing TPB350 and LiTFSI salt in the THF solvent for 4 h. The THF solvent was evaporated under a N_2 atmosphere at room temperature. The blends were then dried in a vacuum oven for 48 h at 50 °C. Four electrolyte compositions were prepared with varying ratios of Li^+ to ethylene oxide (EO) repeat units (Table 1).

Table 1. Ionic Conductivity of TPB350/LiTFSI as a Function of the Salt Content and Temperature

	σ (S cm^{-1})			
EO/Li^+	25 °C	40 °C	55 °C	70 °C
5:1	1.0×10^{-3}	1.2×10^{-3}	1.3×10^{-3}	1.5×10^{-3}
15:1	1.4×10^{-3}	1.5×10^{-3}	1.5×10^{-3}	1.7×10^{-3}
25:1	1.6×10^{-3}	1.8×10^{-3}	1.9×10^{-3}	1.9×10^{-3}
35:1	2.1×10^{-3}	2.5×10^{-3}	3.4×10^{-3}	3.9×10^{-3}

The ionic conductivity values of TPB350/LiTFSI complexes are listed in Table 1. Interestingly, the ionic conductivity was higher than 10^{-3} S cm^{-1} over a wide range of salt contents at 25 °C (Figure 3). The reported ionic conductivity values are similar to the electrolytes containing anion-trapping boron moieties reported in the literature.[35] The glass transition temperatures of the TPB350/LiTFSI electrolytes are given in Table 2. The pure TPB350 shows a glass transition temperature of −71 °C. The T_g increases with an increasing salt content. The increasing T_g can be attributed to the formation of a pseudocross-linked structure because of ion−dipole interaction. However, the effect of the rising T_g on the TPB350/LiTFSI is relatively minor compared to the poly(siloxane) and the poly(phosphazene) electrolytes.[25,26] A plausible explanation for this observation is that decreasing ionic aggregation results in less of an effect on the segmental motion of the polymers, thus lowering the increase in the glass transition temperature.

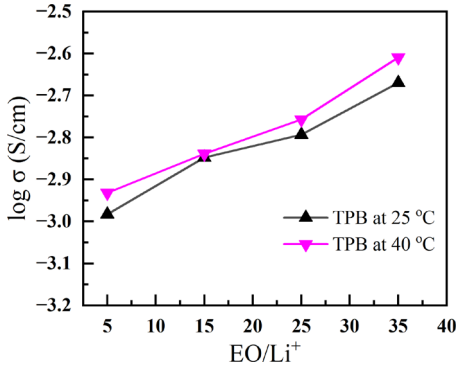

Figure 3. Ionic conductivities of the TPB350/LiTFSI electrolytes at [EO]:[Li^+] ratios of 5, 15, 25, and 35 as a function of temperature.

Table 2. Glass Transition Temperature (T_g) as a Function of the Salt Content for the TPB350/LiTFSI Electrolytes

polymer electrolyte	EO/Li^+ ratio	glass transition temperature (T_g)
TPB350 pure	0	−71 °C
TPB350/LiTFSI	35:1	−67 °C
TPB350/LiTFSI	25:1	−56 °C
TPB350/LiTFSI	15:1	−49 °C
TPB350/LiTFSI	5:1	−43 °C

We believe that the behavior of the TPB350/LiTFSI electrolytes is attributed to the role that the boron atom plays within the matrix. In the TPB350/LITFSI electrolytes, both the anion and the cation interact with the polymer structure, effectively increasing the distance between the anion and the cation. The TPB350 thus functions as an ion separator, and this, in turn, plausibly decreases ionic aggregation. Our modeling study predicted that this may be the effect of incorporating a boron atom within the structure, i.e., the prediction was that the bond length between Li^+ and TFSI would increase. The increased bond length would decrease the electrostatic interactions and thus reduce the level of aggregation, resulting in a more significant fraction of the dissolved ions acting as charge carriers. The modeling prediction was an approximate decrease of 29 kcal/mol for the electrostatic interaction for the boron-containing structure compared with the structure without the boron.

The ion separator function is possible because the anion and cation simultaneously interact with the TPB350 structure (Figure 1). The computational methods predicted the interaction of $TFSI^-$ with TPB350 and were validated by FT-IR experiments.

https://doi.org/10.1021/acsomega.4c01051
ACS Omega 2025, 10, 127−133

The infrared spectra of the TPB350/LiTFSI were simulated using the first-principles density functional theory within the electric field linear response formalism in the CASTEP code.[39] Theoretically, infrared absorption intensities are described using a dynamic matrix known as Hessian and Born effective charges. The Born effective charge of an ion is the partial derivative of the macroscopic polarization concerning a periodic displacement of all of the periodic images of that ion at zero macroscopic electric fields. The Born effective charge tensor is calculated within the linear response formalism by applying a Gonze approximation.[40−42] The Perdew−Burke−Ernzerhof (PBE) parametrization of the generalized gradient approximation (GGA) was used in the calculations. A kinetic energy cutoff of 630 eV in the plane-wave basis and appropriate Monkhorst−Pack *k*-points 6 × 6 × 1 were sufficient to converge the grid integration of the charge density and stable conformations. The classical molecular dynamics method carried out the initial search for stable structures. The obtained local energy-minimum structures were optimized through first-principles calculations with forces less than 0.001 eV/A. For IR spectroscopy calculations, norm-conserving pseudopotentials were employed. Optimizing atomic positions proceeds until the change in energy is less than 1×10^{-6} eV per cell.

The interaction between the boron centers and the anion (TFSI) results in a strong electron supply and increases the B−C bond strength. Stretching frequency changes occur with the B−C bond's strength upon interaction with a donor. Our results show that the B−C bond stretched up to 1.59 Å from its initial value of 1.46 Å after interacting with the TFSI, while the B−C bond stretched up to 1.61 Å from its initial value of 1.46 Å in the absence of TFSI (Figure 4). The wavenumbers

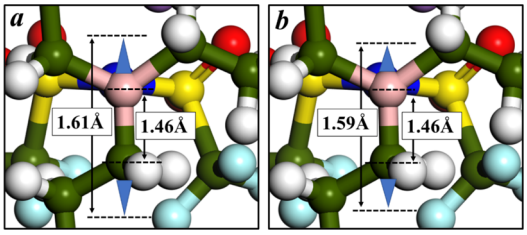

Figure 4. Illustration of the changes in C−B bond stretching in the Lewis-acidic (PEO with boron centers) polymer matrices with (a) and without (b) LiTFSI. Pink, green, white, and blue represent boron, carbon, hydrogen, and nitrogen, respectively.

are proportional to energy, and the angstrom is inversely proportional to energy. In the IR, a blueshift in the bond frequency corresponds to an increased frequency or shift to higher wavenumbers. A redshift indicates a decrease in the frequency or shifts to lower wavenumbers. We observe a change in absorption to the blue part of the spectrum (a blueshift), indicating a population of higher frequency transitions (1040 to 1053 cm^{-1}) (Figure 5a,b). The vibrational analysis was carried out by importing a Hessian matrix from the calculation. Vibrational mode frequencies and infrared intensities were displayed by requesting an electric field response calculation.

4. CONCLUSIONS

In conclusion, we have shown that computational modeling can be utilized to focus on specific design requirements to synthesize new structures for the development of promising electrolytes for lithium batteries. Computational results highlight the value of integrating acidic boron and basic oxygen atoms into the TPB350 structure. Within the TPB350/LiTFSI matrix, both the cations and the anions were interacting with the TPB structure, and this result is TPB350 acting as an ion separator, i.e., increasing the bond length between the anion and cation, thus decreasing the electrostatic interaction. The interaction of the $TFSI^-$ anion with the TPB350 was predicted by computational modeling and validated by experimental FT-IR studies. The observed ionic conductivities of the TPB/LiTFSI electrolytes were greater than 10^{-3} S cm^{-1} at room temperature over a large salt concentration range, making the system very promising as an electrolyte for lithium batteries. The report suggests the tremendous potential of structures containing acidic and basic sites as promising electrolytes for lithium-ion polymer batteries.

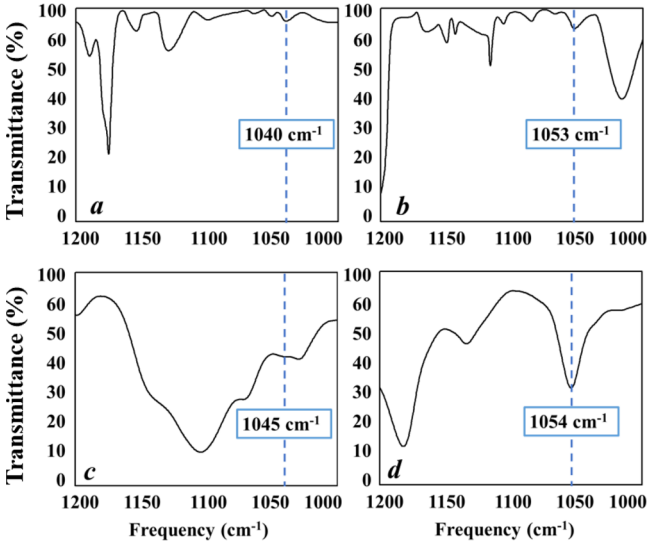

Figure 5. Simulated IR spectra showing peaks of the C−B bond at 1040 cm^{-1} in (a) pure triglyme boron and at 1053 cm^{-1} in (b) blended triglyme boron and experimental FT-IR spectra showing peaks of C−B at 1045 cm^{-1} in (c) pure TPB350 and 1054 cm^{-1} in (d) TPB350/LiTFSI.

■ ASSOCIATED CONTENT

Supporting Information

The Supporting Information is available free of charge at https://pubs.acs.org/doi/10.1021/acsomega.4c01051.

Additional sample characterization and theoretical calculation results using dispersion-corrected density functional theory (PDF)

■ AUTHOR INFORMATION

Corresponding Authors

Xiao-Qian Wang − *Department of Chemistry, Department of Physics, and Center for Functional Nanoscale Materials, Clark Atlanta University, Atlanta, Georgia 30314, United States*; Email: xwang@cau.edu

Ishrat Khan − *Department of Chemistry, Department of Physics, and Center for Functional Nanoscale Materials, Clark Atlanta University, Atlanta, Georgia 30314, United*

https://doi.org/10.1021/acsomega.4c01051
ACS Omega 2025, 10, 127−133

States; orcid.org/0000-0002-4293-8051; Email: ikhan@cau.edu

Authors

Zuhair Hawsawi − *Department of Chemistry, Department of Physics, and Center for Functional Nanoscale Materials, Clark Atlanta University, Atlanta, Georgia 30314, United States*

Ahmed Alzharani − *Department of Chemistry, Department of Physics, and Center for Functional Nanoscale Materials, Clark Atlanta University, Atlanta, Georgia 30314, United States*

Duminda Samarakoon − *Department of Chemistry, Department of Physics, and Center for Functional Nanoscale Materials, Clark Atlanta University, Atlanta, Georgia 30314, United States*

Amal Abdulrahman − *Department of Chemistry, Department of Physics, and Center for Functional Nanoscale Materials, Clark Atlanta University, Atlanta, Georgia 30314, United States*

TaVeion Taylor − *Department of Chemistry, Department of Physics, and Center for Functional Nanoscale Materials, Clark Atlanta University, Atlanta, Georgia 30314, United States*

Md. Hanif Uddin − *Department of Chemistry, Department of Physics, and Center for Functional Nanoscale Materials, Clark Atlanta University, Atlanta, Georgia 30314, United States*

William Gladney − *Department of Chemistry, Department of Physics, and Center for Functional Nanoscale Materials, Clark Atlanta University, Atlanta, Georgia 30314, United States*

Complete contact information is available at: https://pubs.acs.org/10.1021/acsomega.4c01051

Author Contributions

The manuscript was written with contributions from all authors. IK, AA, ZH, AA, and MHU performed synthesis, characterization, and property evaluation. WG and TT carried out structural characterization. DS and XQW carried out theoretical calculations.

Notes

The authors declare no competing financial interest.

■ ACKNOWLEDGMENTS

The authors gratefully acknowledge support for the research from grants from the National Science Foundation program HRD-11137751 and DMR-2122147 and the US Army Research Office WN911NF2010272.

■ REFERENCES

(1) Tan, S.-J.; Zeng, X.-X.; Ma, Q.; Wu, X.-W.; Guo, Y.-G. Recent Advancements in Polymer-Based Composite Electrolytes for Rechargeable Lithium Batteries. *Electrochemical Energy Reviews* **2018**, *1* (2), 113−138.

(2) Cheng, X.; Pan, J.; Zhao, Y.; Liao, M.; Peng, H. Gel Polymer Electrolytes for Electrochemical Energy Storage. *Adv. Energy Mater.* **2018**, *8* (7), 1702184.

(3) Scrosati, B.; Croce, F.; Appetecchi, G. B.; Persi, L. Nano-composite polymer electrolytes for lithium batteries. *Nature* **1998**, *394*, 456.

(4) Goodenough, J. B.; Park, K.-S. The Li-Ion Rechargeable Battery: A Perspective. *J. Am. Chem. Soc.* **2013**, *135* (4), 1167−1176.

(5) Scrosati, B.; Garche, J. Lithium Batteries: Status, Prospects and Future. *J. Power Sources* **2010**, *195* (9), 2419−2430.

(6) Mai, T.; Sandor, D.; Wiser, R.; Schneider, T.Renewable Electricity Futures Study: Executive Summary. *Nat. Renewable Energy Lab.* **2012** .

(7) Ziegler, M. S.; Mueller, J. M.; Pereira, G. D.; Song, J.; Ferrara, M.; Chiang, Y.-M.; Trancik, J. E. Storage Requirements and Costs of Shaping Renewable Energy Toward Grid Decarbonization. *Joule* **2019**, *3*, 2134−2153.

(8) Kim, T.; Song, W.; Son, D. Y.; Ono, L. K.; Qi, Y. Lithium-ion batteries: outlook on present, future, and hybridized technologies. *J. Mater. Chem. A* **2019**, *7*, 2942−2964.

(9) Balaish, M.; Kraytsberg, A.; Ein-Eli, Y. A critical review on lithium-air battery electrolytes. *Phys. Chem. Chem. Phys.* **2014**, *16* (7), 2801−2822.

(10) Kalhoff, J.; Eshetu, G. G.; Bresser, D.; Passerini, S. Safer Electrolytes for Lithium-Ion Batteries: State of the Art and Perspectives. *ChemSusChem* **2015**, *8* (13), 2154−2175.

(11) Girishkumar, G.; McCloskey, B.; Luntz, A. C.; Swanson, S.; Wilcke, W. Lithium−Air Battery: Promise and Challenges. *J. Phys. Chem. Lett.* **2010**, *1* (14), 2193−2203.

(12) Zha, Z.; Shen, C.; Wang, D.; Han, W.-Q. Review on Air Cathode in Li-Air Batteries. *J. Technol. Innovations Renewable Energy* **2013**, 293.

(13) Scherson, D.; Cali, L.; Sarangapani, S. *A Polymer Electrolyte-Based Rechargeable Lithium/Oxygen Battery A Portable Oxygen Concentrator for Wound Healing Applications This Content Was Downloaded from IP Address*; 1996; Vol. *143*.

(14) Chabanel, M. Ionic Aggregates of 1−1 Salts in Nonaqueous Solutions: Structure, Thermodynamics and Solvation. *Pure Appl. Chem.* **1990**, *62* (1), 35−46.

(15) Yu, Z.; Curtiss, L. A.; Winans, R. E.; Zhang, Y.; Li, T.; Cheng, L. Asymmetric Composition of Ionic Aggregates and the Origin of High Correlated Transference Number in Water-in-Salt Electrolytes. *J. Phys. Chem. Lett.* **2020**, *11* (4), 1276−1281.

(16) Fenton, D. E.; Parker, J. M.; Wright, P. V. Complexes of Alkali Metal Ions with Poly(Ethylene Oxide). *Polymer (Guildf)* **1973**, *14* (11), 589.

(17) Wright, P. V. Developments in Polymer Electrolytes for Lithium Batteries. *MRS Bull.* **2002**, *27* (8), 597−602.

(18) Xue, Z.; He, D.; Xie, X. Poly(Ethylene Oxide)-Based Electrolytes for Lithium-Ion Batteries. *J. Mater. Chem. A Mater.* **2015**, *3* (38), 19218−19253.

(19) Khan, I. M.; Yuan, Y.; Fish, D.; Wu, E.; Smid, J. Comblike polysiloxanes with oligo(oxyethylene) side chains. Synthesis and properties. *Macromolecules* **1988**, *21* (9), 2684−2689.

(20) Tsuchida, E.; Ohno, H.; Tsunemi, K.; Kobayashi, N. Lithium Ionic Conduction in Poly (Methacrylic Acid)-Poly (Ethylene Oxide) Complex Containing Lithium Perchlorate. *Solid State Ion* **1983**, *11* (3), 227−233.

(21) Rocco, A. M.; da Fonseca, C. P.; Pereira, R. P. A Polymeric Solid Electrolyte Based on a Binary Blend of Poly(Ethylene Oxide), Poly(Methyl Vinyl Ether-Maleic Acid) and LiClO 4. *Polymer (Guildf)* **2002**, *43* (13), 3601−3609.

(22) Li, J.; Khan, I. M. Highly Conductive Solid Polymer Electrolytes Prepared by Blending High Molecular Weight Poly (Ethylene Oxide), Poly (2-or 4-Vinylpyridine), and Lithium Perchlorate. *Macromolecules* **1993**, *26*, 4544−4550.

(23) Yao, P.; Yu, H.; Ding, Z.; Liu, Y.; Lu, J.; Lavorgna, M.; Wu, J.; Liu, X. Review on Polymer-Based Composite Electrolytes for Lithium Batteries. *Front Chem.* **2019**, *7*, 522.

(24) Bocharova, V.; Sokolov, A. P. Perspectives for Polymer Electrolytes: A View from Fundamentals of Ionic Conductivity. *Macromolecules.* **2020**, *53*, 4141−4157.

(25) Blonsky, P. M.; Shriver, D. F.; Austin, P.; Allcock, H. R. Austin, Allcock, Polyphosphazene Solid Electrolytes. *J. Am. Chem. Soc.* **1984**, *106*, 6854−6855.

(26) Fish, D.; Khan, I. M.; Smid, J. Conductivity of Solid Complexes of Lithium Perchlorate with Poly{[ω-Methoxyhexa(Oxyethylene)-

Ethoxy]Methylsiloxane}†. *Makromolekulare Chemie, Rapid Communications* **1986**, *7* (3), 115−120.
(27) Wang, Q.; Zhang, H.; Cui, Z.; Zhou, Q.; Shangguan, X.; Tian, S.; Zhou, X.; Cui, G. Siloxane-Based Polymer Electrolytes for Solid-State Lithium Batteries. *Energy Storage Mater.* **2019**, *23*, 466−490.
(28) Hooper, R.; Lyons, L. J.; Moline, D. A.; West, R. A Highly Conductive Solid-State Polymer Electrolyte Based on a Double-Comb Polysiloxane Polymer with Oligo(Ethylene Oxide) Side Chains. *Organometallics* **1999**, *18* (17), 3249−3251.
(29) Zugmann, S.; Fleischmann, M.; Amereller, M.; Gschwind, R. M.; Wiemhöfer, H. D.; Gores, H. J. Measurement of Transference Numbers for Lithium Ion Electrolytes via Four Different Methods, a Comparative Study. *Electrochim. Acta* **2011**, *56* (11), 3926−3933.
(30) BRUCE, P. Conductivity and Transference Number Measurements on Polymer Electrolytes. *Solid State Ion* **1988**, *28−30* (PART 2), 918−922.
(31) Porcarelli, L.; Shaplov, A. S.; Bella, F.; Nair, J. R.; Mecerreyes, D.; Gerbaldi, C. Single-Ion Conducting Polymer Electrolytes for Lithium Metal Polymer Batteries That Operate at Ambient Temperature. *ACS Energy Lett.* **2016**, *1* (4), 678−682.
(32) Rolland, J.; Poggi, E.; Vlad, A.; Gohy, J. F. Single-Ion Diblock Copolymers for Solid-State Polymer Electrolytes. *Polymer (Guildf)* **2015**, *68*, 344−352.
(33) Luo, G.; Yuan, B.; Guan, T.; Cheng, F.; Zhang, W.; Chen, J. Synthesis of Single Lithium-Ion Conducting Polymer Electrolyte Membrane for Solid-State Lithium Metal Batteries. *ACS Appl. Energy Mater.* **2019**, *2* (5), 3028−3034.
(34) Miller, T. F.; Wang, Z.-G.; Coates, G. W.; Balsara, N. P. Designing Polymer Electrolytes for Safe and High Capacity Rechargeable Lithium Batteries. *Acc. Chem. Res.* **2017**, *50* (3), 590−593.
(35) Shim, J.; Lee, J. S.; Lee, J. H.; Kim, H. J.; Lee, J.-C. Gel Polymer Electrolytes Containing Anion-Trapping Boron Moieties for Lithium-Ion Battery Applications. *ACS Appl. Mater. Interfaces* **2016**, *8* (41), 27740−27752.
(36) Mehta, M. A.; Fujinami, T. Li $^{+}$ Transference Number Enhancement in Polymer Electrolytes by Incorporation of Anion Trapping Boroxine Rings into the Polymer Host. *Chem. Lett.* **1997**, *26* (9), 915−916.
(37) Kato, Y.; Yokoyama, S.; Ikuta, H.; Uchimoto, Y.; Wakihara, M. Thermally Stable Polymer Electrolyte Plasticized with PEG-Borate Ester for Lithium Secondary Battery. *Electrochem. Commun.* **2001**, *3* (3), 128−130.
(38) Reddy, Y. G.; Chary, A. S.; Reddy, S. N., Ionic Conductivity Study by Two Probe Method on (1-X)Pb(No3)2:Xceo2 Composite Solid Electrolyte. *Mater. Sci. Rs. India*; *12* (2). http://www.materialsciencejournal.org/?p=3649.
(39) Payne, M. C.; Teter, M. P.; Allan, D. C.; Arias, T. A.; Joannopoulos, J. D. Iterative Minimization Techniques for Ab Initio Total-Energy Calculations: Molecular Dynamics and Conjugate Gradients. *Rev. Mod. Phys.* **1992**, *64*, 1045.
(40) Parr, R. G.; Yang, W.; Yang, W. *Density-Functional Theory of Atoms and Molecules*; Oxford University Press: New York, 1994.
(41) Perdew, J. P.; Burke, K.; Ernzerhof, M. Generalized Gradient Approximation Made Simple. *Phys. Rev. Lett.* **1996**, *77*, 3865−3868.
(42) Tkatchenko, A.; Scheffler, M. Accurate Molecular van Der Waals Interactions from Ground-State Electron Density and Free-Atom Reference Data. *Phys. Rev. Lett.* **2009**, *102* (7), No. 073005.

https://doi.org/10.1021/acsomega.4c01051
ACS Omega 2025, 10, 127−133